A modified Drude-Born-Fedorov model for isotropic chiral media, obtained by finite scale homogenization

Sjöberg, Daniel

2008

CODEN:LUTEDX/(TEAT-7167)/1-10/(2008)

A modified Drude-Born-Fedorov model for isotropic chiral media, obtained by finite scale homogenization

Daniel Sjöberg

Electromagnetic Theory
Department of Electrical and Information Technology
Lund University
Sweden

Daniel Sjöberg
Daniel.Sjoberg@eit.lth.se

Department of Electrical and Information Technology
Electromagnetic Theory
P.O. Box 118
SE-221 00 Lund
Sweden

Editor: Gerhard Kristensson

Abstract

Isotropic chiral media can be modeled in several ways. We show that when realizing such a medium from spiral inclusions with real permittivities and permeabilities in a periodic structure, a modified Drude-Born-Fedorov model is obtained. This model equals the original Born model for small wave vectors, but the strength of the chirality depends on the propagation direction. The effective parameters are calculated by an unbiased finite scale homogenization method, which in principle could generate any model.

1 Introduction

Chiral media are interesting from a homogenization point of view, since they are difficult to treat rigorously with classical methods. In 1914, Lindman created an artificial medium composed of small metal coils, all wound the same way, embedded in a background material [16, 17]. The resulting material exhibited different propagation speed for left and right hand circularly polarized waves, respectively. Many others have followed, and a similar effect exists for visible light in sugar solutions, where the different refractive indices for left and right circular polarized light is explained by the fact that the sugar molecules found in nature have a handedness, which introduces a preference for left or right. For more information on chiral media we refer to the books [13, 15] and references therein.

An interesting fact about chiral materials is that there is some arbitrariness in how to model the chirality. Essentially, three different models can be identified: the Post, Tellegen, and Drude-Born-Fedorov model, respectively. For time-harmonic fields, all these models can be transformed into each other, and one may ask if any model is more natural than the others. In this contribution, we show that within a particular framework of homogenization, the Drude-Born-Fedorov model seems more natural than the others.

Homogenization is the science of calculating effective material parameters for composite materials, based on knowledge of the material parameters of the components and the microscopic structure in which the components are mixed. We refer to the books [2, 6, 10, 18, 24] and references therein for a review of this huge field. The problem with classical homogenization is that in order to formulate rigorous mathematical results, it is assumed that the applied wavelength is infinitely large compared to the unit cell. In this limit, the electric and magnetic fields decouple, and it seems there can be no chiral effects.

In recent years, new formalisms which provide a framework of finite scale homogenization have been developed [7, 19–23]. These provide a window of opportunity to rigorously calculate chiral effects in composite media. In this paper, we use results from [23] to prove that if the permittivity and permeability of the component materials involved have so small losses that they can be considered as real valued parameters, only the Drude-Born-Fedorov model can be considered as a reasonable choice. The argument is surprisingly simple, and rests on a simple symmetry relation for Maxwell's equations. This symmetry disappears as soon as a finite conductivity

is introduced in the material description, but reappears when the conductivity is infinite, which is the perfect electric conductor (PEC) case.

2 Dispersion relations and band plots

It is common to model heterogeneous materials by assuming the microstructure is periodic, since this allows a detailed analysis of the microscopic geometry based on periodic boundary conditions for the unit cell U. Once the unit cell U has been specified, a reciprocal unit cell U' is also defined (the first Brillouin zone) [12]. Using the Floquet-Bloch representation an arbitrary square integrable field $\boldsymbol{E}(\boldsymbol{x})$ can be written [3, 9, 23],

$$\boldsymbol{E}(\boldsymbol{x}) = \frac{1}{|U'|}\int_{U'} \mathrm{e}^{\mathrm{i}\boldsymbol{k}\cdot\boldsymbol{x}}\widetilde{\boldsymbol{E}}(\boldsymbol{x},\boldsymbol{k})\,\mathrm{d}\boldsymbol{k} \tag{2.1}$$

The field $\widetilde{\boldsymbol{E}}(\boldsymbol{x},\boldsymbol{k})$ is called the Bloch amplitude, and is U-periodic in $\boldsymbol{x}$ whereas the field $\mathrm{e}^{\mathrm{i}\boldsymbol{k}\cdot\boldsymbol{x}}\widetilde{\boldsymbol{E}}(\boldsymbol{x},\boldsymbol{k})$ is U'-periodic in $\boldsymbol{k}$. A typical effect when using this representation is the transformation of the nabla operator, $\nabla \to \nabla + \mathrm{i}\boldsymbol{k}$. It is shown in [23], that the following eigenvalue problem contains the pertinent information of the problem when the material consists of only real, symmetric permittivity matrix $\boldsymbol{\epsilon}(\boldsymbol{x})$ and real, symmetric permeability matrix $\boldsymbol{\mu}(\boldsymbol{x})$, which are both assumed U-periodic:

$$\begin{pmatrix} \mathbf{0} & -(\nabla+\mathrm{i}\boldsymbol{k})\times\mathbf{I} \\ (\nabla+\mathrm{i}\boldsymbol{k})\times\mathbf{I} & \mathbf{0} \end{pmatrix}\begin{pmatrix}\widetilde{\boldsymbol{E}}_n \\ \widetilde{\boldsymbol{H}}_n\end{pmatrix} = \mathrm{i}\omega_n\begin{pmatrix}\boldsymbol{\epsilon}(\boldsymbol{x}) & \mathbf{0} \\ \mathbf{0} & \boldsymbol{\mu}(\boldsymbol{x})\end{pmatrix}\begin{pmatrix}\widetilde{\boldsymbol{E}}_n \\ \widetilde{\boldsymbol{H}}_n\end{pmatrix} \tag{2.2}$$

where $\boldsymbol{x} \in U$ and $\boldsymbol{k} \in U'$. When the unit cell contains a PEC region Ω (such as the coils in Lindman's experiment), the problem is modified so that only space vectors outside the PEC region, $\boldsymbol{x} \in U \setminus \Omega$, are considered. We also require the boundary condition that electric fields tangential to the surface of Ω are zero, *i.e.*, $\hat{\boldsymbol{n}} \times \widetilde{\boldsymbol{E}} = \mathbf{0}$ where $\hat{\boldsymbol{n}}$ is the normal to $\partial\Omega$. The same conclusions can then be made for the PEC case as when the entire unit cell is filled with finite material parameters $\boldsymbol{\epsilon}(\boldsymbol{x})$ and $\boldsymbol{\mu}(\boldsymbol{x})$.

It is shown in [23] that the eigenvalue problem (2.2) is well posed, and the solutions can be used as a basis in a properly defined function space for Maxwell's equations. The eigenvalues ω_n are real, and form a nondecreasing sequence

$$0 \le \omega_1^2 \le \omega_2^2 \le \cdots \tag{2.3}$$

Since $\boldsymbol{k} \in U'$ is a free parameter, the eigenvalue problem (2.2) defines ω_n as a function of $\boldsymbol{k}$, which is the dispersion relation $\omega_n = W_n(\boldsymbol{k})$.

For each eigenvector $[\widetilde{\boldsymbol{E}}_n, \widetilde{\boldsymbol{H}}_n]^{\mathrm{T}}$ with eigenvalue ω_n, there is a corresponding eigenvector $[\widetilde{\boldsymbol{E}}_n, -\widetilde{\boldsymbol{H}}_n]^{\mathrm{T}}$ with eigenvalue $-\omega_n$. This is shown by

$$\begin{aligned}\begin{pmatrix} \mathbf{0} & -(\nabla+\mathrm{i}\boldsymbol{k})\times\mathbf{I} \\ (\nabla+\mathrm{i}\boldsymbol{k})\times\mathbf{I} & \mathbf{0} \end{pmatrix}\begin{pmatrix}\widetilde{\boldsymbol{E}}_n \\ -\widetilde{\boldsymbol{H}}_n\end{pmatrix} &= \begin{pmatrix}(\nabla+\mathrm{i}\boldsymbol{k})\times\widetilde{\boldsymbol{H}}_n \\ (\nabla+\mathrm{i}\boldsymbol{k})\times\widetilde{\boldsymbol{E}}_n\end{pmatrix} \\ &= \begin{pmatrix}-\mathrm{i}\omega_n\boldsymbol{\epsilon}(\boldsymbol{x})\cdot\widetilde{\boldsymbol{E}}_n \\ \mathrm{i}\omega_n\boldsymbol{\mu}(\boldsymbol{x})\cdot\widetilde{\boldsymbol{H}}_n\end{pmatrix} = -\mathrm{i}\omega_n\begin{pmatrix}\boldsymbol{\epsilon}(\boldsymbol{x}) & \mathbf{0} \\ \mathbf{0} & \boldsymbol{\mu}(\boldsymbol{x})\end{pmatrix}\begin{pmatrix}\widetilde{\boldsymbol{E}}_n \\ -\widetilde{\boldsymbol{H}}_n\end{pmatrix}\end{aligned} \tag{2.4}$$

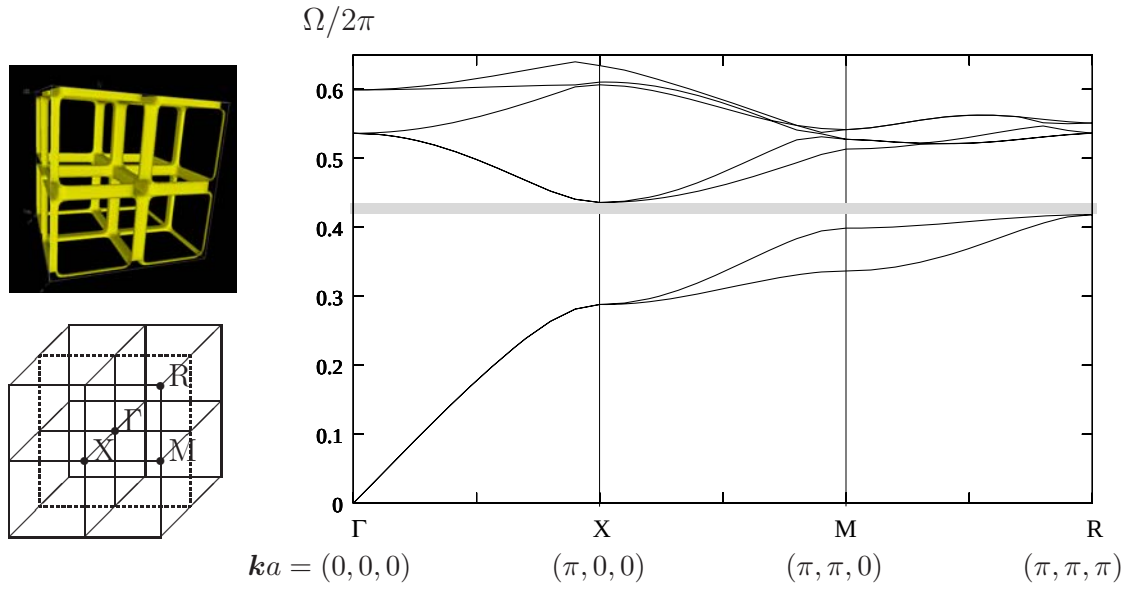

Figure 1: Plot of a typical band structure. The eigenvalues $\Omega_n = ac^{-1}\omega_n$ for the geometry in the upper left figure (normalized unit cell $a^{-1}U =]0,1[^3$ where a is the size of the physical unit cell U) are depicted as functions of the normalized wave vector $\boldsymbol{k}a$ in the reciprocal unit cell $aU' =]-\pi,\pi[^3$ in the lower left figure. The thin grey strip is a band gap, where there are no eigenvalues regardless of the wave vector. Thus, in this frequency interval there can exist no fixed frequency solutions to Maxwell's equations, and for frequencies below this band gap, only two modes contribute to the electric field. The calculations are made with the program described in [11], and the scaffold geometry is taken from [8]. The thickness of the bars is 20% of the unit cell, and the permittivity in the bars is 12.96.

where we used (2.2) to arrive at the second line. This demonstrates that it is sufficient to consider only dispersion relations corresponding to positive ω_n. A typical example of dispersion relations for a specific geometry is given in Figure 1.

3 Calculation of effective material parameters

In [22, 23], it is shown that a periodic heterogeneous material can be replaced by a homogeneous, effective material when the wavelength is large enough. More precisely, the condition can be written as

$$2\pi\frac{a}{\lambda_0} < \frac{\pi - 1}{\|\boldsymbol{\epsilon}(\cdot)/\epsilon_0 - 1\| + 1} \tag{3.1}$$

for non-magnetic media, where λ_0 is the vacuum wavelength, ϵ_0 is the permittivity of vacuum, and a is the length of the unit cell. Note that this does not require the unit cell to be infinitely small compared to the vacuum wavelength. For a fixed $\boldsymbol{k} \in U'$, the effective material parameters can be expressed in terms of the mean values of

the eigenvectors corresponding to the four eigenvalues with smallest absolute value. These are the dispersion relations $W_n(\boldsymbol{k})$ which go to zero as $\boldsymbol{k} \to \boldsymbol{0}$ in Figure 1, and are termed acoustic modes in [23]. The relation defining the parameters is

$$\begin{pmatrix} \langle \widetilde{\boldsymbol{D}} \rangle \\ \langle \widetilde{\boldsymbol{B}} \rangle \end{pmatrix} = \begin{pmatrix} \boldsymbol{\epsilon}_{\text{eff}} & \boldsymbol{\xi}_{\text{eff}} \\ \boldsymbol{\zeta}_{\text{eff}} & \boldsymbol{\mu}_{\text{eff}} \end{pmatrix} \begin{pmatrix} \langle \widetilde{\boldsymbol{E}} \rangle \\ \langle \widetilde{\boldsymbol{H}} \rangle \end{pmatrix} \tag{3.2}$$

where $\langle \widetilde{\boldsymbol{D}} \rangle$ denotes the mean value of the Bloch amplitude of the electric flux density over the unit cell U etc. The explicit formula for the effective material parameters in terms of the acoustic modes is [23]

$$\begin{pmatrix} \boldsymbol{\epsilon}_{\text{eff}} & \boldsymbol{\xi}_{\text{eff}} \\ \boldsymbol{\zeta}_{\text{eff}} & \boldsymbol{\mu}_{\text{eff}} \end{pmatrix} = \sum_{n=1}^{4} \frac{\begin{pmatrix} \langle \boldsymbol{\epsilon} \cdot \widetilde{\boldsymbol{E}}_n \rangle \\ \langle \boldsymbol{\mu} \cdot \widetilde{\boldsymbol{H}}_n \rangle \end{pmatrix} \begin{pmatrix} \langle \boldsymbol{\epsilon} \cdot \widetilde{\boldsymbol{E}}_n \rangle^* \\ \langle \boldsymbol{\mu} \cdot \widetilde{\boldsymbol{H}}_n \rangle^* \end{pmatrix}}{\langle \boldsymbol{\epsilon} \cdot \widetilde{\boldsymbol{E}}_n \rangle^* \cdot \langle \widetilde{\boldsymbol{E}}_n \rangle + \langle \boldsymbol{\mu} \cdot \widetilde{\boldsymbol{H}}_n \rangle^* \cdot \langle \widetilde{\boldsymbol{H}}_n \rangle} \tag{3.3}$$

where the numerator should be understood as a dyadic product. The parameters $\boldsymbol{\xi}_{\text{eff}}$ and $\boldsymbol{\zeta}_{\text{eff}}$ model the possible direct coupling between electric and magnetic fields in the constitutive relation. Denoting the normalization factor by $1/(\langle \boldsymbol{\epsilon} \cdot \widetilde{\boldsymbol{E}}_n \rangle^* \cdot \langle \widetilde{\boldsymbol{E}}_n \rangle + \langle \boldsymbol{\mu} \cdot \widetilde{\boldsymbol{H}}_n \rangle^* \cdot \langle \widetilde{\boldsymbol{H}}_n \rangle) = A_n$, we obtain for each of the matrices $\boldsymbol{\epsilon}_{\text{eff}}$, $\boldsymbol{\xi}_{\text{eff}}$, $\boldsymbol{\zeta}_{\text{eff}}$, and $\boldsymbol{\mu}_{\text{eff}}$,

$$\boldsymbol{\epsilon}_{\text{eff}} = \sum_{n=1}^{4} A_n \langle \boldsymbol{\epsilon} \cdot \widetilde{\boldsymbol{E}}_n \rangle \langle \boldsymbol{\epsilon} \cdot \widetilde{\boldsymbol{E}}_n \rangle^* \tag{3.4}$$

$$\boldsymbol{\xi}_{\text{eff}} = \sum_{n=1}^{4} A_n \langle \boldsymbol{\epsilon} \cdot \widetilde{\boldsymbol{E}}_n \rangle \langle \boldsymbol{\mu} \cdot \widetilde{\boldsymbol{H}}_n \rangle^* \tag{3.5}$$

$$\boldsymbol{\zeta}_{\text{eff}} = \sum_{n=1}^{4} A_n \langle \boldsymbol{\mu} \cdot \widetilde{\boldsymbol{H}}_n \rangle \langle \boldsymbol{\epsilon} \cdot \widetilde{\boldsymbol{E}}_n \rangle^* \tag{3.6}$$

$$\boldsymbol{\mu}_{\text{eff}} = \sum_{n=1}^{4} A_n \langle \boldsymbol{\mu} \cdot \widetilde{\boldsymbol{H}}_n \rangle \langle \boldsymbol{\mu} \cdot \widetilde{\boldsymbol{H}}_n \rangle^* \tag{3.7}$$

We now utilize the property that if $[\widetilde{\boldsymbol{E}}_n, \widetilde{\boldsymbol{H}}_n]^{\text{T}}$ is an eigenvector, then $[\widetilde{\boldsymbol{E}}_n, -\widetilde{\boldsymbol{H}}_n]$ is also an eigenvector. This means

$$\begin{aligned} \boldsymbol{\xi}_{\text{eff}} &= \sum_{n=1}^{4} A_n \langle \boldsymbol{\epsilon} \cdot \widetilde{\boldsymbol{E}}_n \rangle \langle \boldsymbol{\mu} \cdot \widetilde{\boldsymbol{H}}_n \rangle^* \\ &= \sum_{n=1}^{2} A_n \Big(\langle \boldsymbol{\epsilon} \cdot \widetilde{\boldsymbol{E}}_n \rangle \langle \boldsymbol{\mu} \cdot \widetilde{\boldsymbol{H}}_n \rangle^* + \langle \boldsymbol{\epsilon} \cdot \widetilde{\boldsymbol{E}}_n \rangle \langle \boldsymbol{\mu} \cdot (-\widetilde{\boldsymbol{H}}_n) \rangle^* \Big) \equiv \boldsymbol{0} \end{aligned} \tag{3.8}$$

and the same result applies to $\boldsymbol{\zeta}_{\text{eff}}$. Thus, only $\boldsymbol{\epsilon}_{\text{eff}}$ and $\boldsymbol{\mu}_{\text{eff}}$ can be nonzero for a composite material using only real valued component materials (and possibly some PEC inclusion).

We end this section by pointing out that the arguments presented above to prove that $\boldsymbol{\xi}_{\text{eff}} = \boldsymbol{\zeta}_{\text{eff}} = \boldsymbol{0}$ break down when the component materials are lossy. The

	Tellegen	Post	Drude-Born-Fedorov
$\boldsymbol{D} =$	$\epsilon_{\mathrm{T}}\boldsymbol{E} + \zeta\boldsymbol{H}$	$\epsilon_{\mathrm{P}}\boldsymbol{E} + \mathrm{i}\xi\boldsymbol{B}$	$\epsilon(\boldsymbol{E} + \beta\nabla\times\boldsymbol{E})$
$\boldsymbol{B} =$	$\mu_{\mathrm{T}}\boldsymbol{H} - \zeta\boldsymbol{E}$	$\mu_{\mathrm{P}}(\boldsymbol{H} - \mathrm{i}\xi\boldsymbol{E})$	$\mu(\boldsymbol{H} + \beta\nabla\times\boldsymbol{H})$

Table 1: Three different possible descriptions of isotropic chiral media [13, pp. 15–16].

generalization of the eigenvalue problem (2.2) to include a conductivity is

$$\begin{pmatrix} \boldsymbol{\sigma}(\boldsymbol{x}) & -(\nabla + \mathrm{i}\boldsymbol{k})\times\mathbf{I} \\ (\nabla + \mathrm{i}\boldsymbol{k})\times\mathbf{I} & \mathbf{0} \end{pmatrix} \begin{pmatrix} \widetilde{\boldsymbol{E}}_n \\ \widetilde{\boldsymbol{H}}_n \end{pmatrix} = \mathrm{i}\omega_n \begin{pmatrix} \boldsymbol{\epsilon}(\boldsymbol{x}) & \mathbf{0} \\ \mathbf{0} & \boldsymbol{\mu}(\boldsymbol{x}) \end{pmatrix} \begin{pmatrix} \widetilde{\boldsymbol{E}}_n \\ \widetilde{\boldsymbol{H}}_n \end{pmatrix} \tag{3.9}$$

where the electric conductivity matrix $\boldsymbol{\sigma}(\boldsymbol{x})$ is a nonnegative matrix. The introduction of this matrix into the operator directly influences the fundamental properties of the eigenvalue problem, so that the eigenvalues ω_n are no longer real. As is shown in [14], the imaginary part of the eigenvalues is always nonpositive, $\mathrm{Im}(\omega_n) \leq 0$. This implies that if $[\widetilde{\boldsymbol{E}}_n, \widetilde{\boldsymbol{H}}_n]^{\mathrm{T}}$ is an eigenvector, it is no longer guaranteed that $[\widetilde{\boldsymbol{E}}_n, -\widetilde{\boldsymbol{H}}_n]^{\mathrm{T}}$ is an eigenvector.

This means that for lossy component materials, there can very well be a coupling term between electric and magnetic fields in the effective constitutive relations. However, this coupling is expected to be weak for small losses.

4 Different constitutive relations for chiral media

There are three major models that have been used to model isotropic chiral materials, as given in Table 1. For time-harmonic fields in source free regions, the different models can be transformed into each other. If sources are present they may need to be transformed too.

The results in the preceding section implies that the coupling terms between electric and magnetic fields in the Tellegen and Post descriptions must necessarily be zero for the effective material computed by the formula (3.3). This leaves the Drude-Born-Fedorov model as the natural choice for describing chiral materials.

This model has some problems. Since it involves spatial derivatives in the constitutive relation, it is a nonlocal relation. This means special care has to be taken when using the formulation in a scattering problem, where the proper boundary conditions must be applied. Some of these problems are treated in, *e.g.*, [1, 13].

Applying the Floquet-Bloch transformation to the electric part of the Drude-Born-Fedorov model implies

$$\widetilde{\boldsymbol{D}} = \epsilon(\widetilde{\boldsymbol{E}} + \beta(\nabla + \mathrm{i}\boldsymbol{k})\times\widetilde{\boldsymbol{E}}) \tag{4.1}$$

with the mean value over the unit cell U

$$\langle\widetilde{\boldsymbol{D}}\rangle = \epsilon(\mathbf{I} + \beta\mathrm{i}\boldsymbol{k}\times)\,\langle\widetilde{\boldsymbol{E}}\rangle \tag{4.2}$$

since the mean value of any derivative of a periodic field is zero, $\langle \nabla \times \widetilde{\boldsymbol{E}} \rangle = \mathbf{0}$. This implies that chiral effects should appear as a gyrotropic tensor

$$\beta \mathrm{i} \boldsymbol{k} \times = \beta |\boldsymbol{k}| \begin{pmatrix} 0 & -\mathrm{i} & 0 \\ \mathrm{i} & 0 & 0 \\ 0 & 0 & 0 \end{pmatrix} \tag{4.3}$$

where it was assumed that the wave vector is in the z direction, $\boldsymbol{k} = |\boldsymbol{k}| \hat{\boldsymbol{z}}$. This matrix is seen to be hermitian symmetric for real β, which implies there is no loss due to this term, corresponding well to the fact that our composite material is built of lossless components. The same procedure applies to the magnetic fields.

5 Results for a specific microstructure

As a numerical demonstration, spiral inclusions have been implemented in the program described in [11] as depicted in Figure 2. The effective material parameters are computed according to (3.3), and we attempt to fit the following model to the data:

$$\langle \widetilde{\boldsymbol{D}} \rangle = \epsilon (\mathbf{I} - \hat{\boldsymbol{k}} \hat{\boldsymbol{k}} + \beta_1 \mathrm{i} \boldsymbol{k} \times) \langle \widetilde{\boldsymbol{E}} \rangle \tag{5.1}$$

$$\langle \widetilde{\boldsymbol{B}} \rangle = \mu (\mathbf{I} - \hat{\boldsymbol{k}} \hat{\boldsymbol{k}} + \beta_2 \mathrm{i} \boldsymbol{k} \times) \langle \widetilde{\boldsymbol{H}} \rangle \tag{5.2}$$

i.e., an extended Drude-Born-Fedorov model where we allow different β-factors in the electric and magnetic relations, respectively. Note that we must subtract $\hat{\boldsymbol{k}} \hat{\boldsymbol{k}}$ from the three-dimensional identity matrix, since the effective permittivity computed from (3.3) cannot have components in the $\boldsymbol{k}$-direction [23].

The parameters ϵ and β_1 are extracted from the computed $\boldsymbol{\epsilon}_{\text{eff}}$ using the formulas

$$\epsilon = \frac{\operatorname{tr}(\boldsymbol{\epsilon}_{\text{eff}})}{2} \tag{5.3}$$

$$\epsilon \beta_1 = \frac{\operatorname{tr}(\mathrm{i} \boldsymbol{k} \times \boldsymbol{\epsilon}_{\text{eff}})}{2 |\boldsymbol{k}|^2} \tag{5.4}$$

where $\operatorname{tr}(\boldsymbol{\epsilon}_{\text{eff}})$ denotes the trace of the matrix $\boldsymbol{\epsilon}_{\text{eff}}$. It is easy to verify that these formulas are exact if our model (5.1) is true, and since the computations for each fixed $\boldsymbol{k}$ are independent, the computed parameters ϵ and β_1 will in general depend on $\boldsymbol{k}$. The same procedure is applied to calculate the relevant μ and β_2 parameters from $\boldsymbol{\mu}_{\text{eff}}$.

In Figure 2, we plot the geometry of the unit cell, along with the reconstructed parameters ϵ, β_1, μ, β_2, and the approximate relative error in the effective material matrices using these parameters, *i.e.*,

$$\delta_\epsilon = \frac{\| \boldsymbol{\epsilon}'_{\text{eff}} - \boldsymbol{\epsilon}_{\text{eff}} \|}{\| \boldsymbol{\epsilon}_{\text{eff}} \|} \tag{5.5}$$

where $\boldsymbol{\epsilon}_{\text{eff}}$ is the original effective permittivity calculated using (3.3), and $\boldsymbol{\epsilon}'_{\text{eff}}$ is the permittivity calculated using the model (5.1) with the identified parameters ϵ and

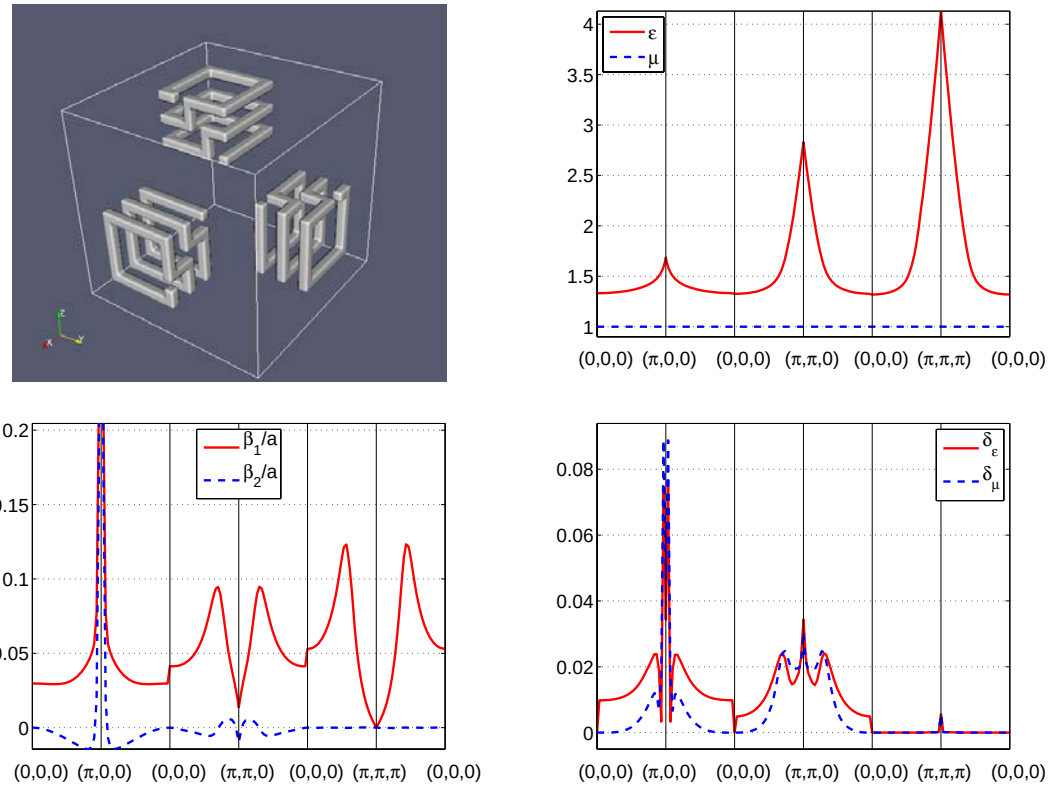

Figure 2: Spiral geometry and the effective ϵ, μ, β_1 and β_2 parameters as computed by (5.3) and (5.4). Only the real part of the parameters is plotted, the imaginary part is at least a factor $3 \cdot 10^{-5}$ less than the real part for each parameter and can be considered as numerical noise. The approximate relative errors δ_ϵ and δ_μ as defined in (5.5) are also plotted. On the horizontal axis are different values of the normalized wave vector $\boldsymbol{k}a$ within the reciprocal unit cell. In the graph for β_1 and β_2, the peaks at $\boldsymbol{k}a = (\pi, 0, 0)$ have been truncated, the top value is 0.78 for both curves. The resolution of the unit cell is $128 \times 128 \times 128$ pixels, and the results are close to identical if the resolution $64 \times 64 \times 64$ is used instead. The material in the spirals is nonmagnetic with a permittivity of 100.

β_1 calculated from (5.3) and (5.4). The matrix norm used is the largest singular value norm, and the corresponding error δ_μ for the permeability is also shown. It is seen that the error is below 2.5% except for $\boldsymbol{k}a$ close to $(\pi, 0, 0)$ and $(\pi, \pi, 0)$. The error is almost entirely due to the structure not being completely isotropic, since the spirals are slightly asymmetric. If we measure only the error concerning the chirality, *i.e.*, the fit of the imaginary parts of $\boldsymbol{\epsilon}_{\text{eff}}$ and $\boldsymbol{\mu}_{\text{eff}}$, the approximate relative error level drops to below $3 \cdot 10^{-6}$ for all $\boldsymbol{k}$.

Studying the results in Figure 2, it is clearly seen that the factors β_1 and β_2 are in general not equal. In particular, we see that for small wave vectors we have

$$\beta_1 \to \beta_0 \neq 0 \quad \text{and} \quad \beta_2 \to 0 \quad \text{when} \quad |\boldsymbol{k}| \to 0 \tag{5.6}$$

where the value β_0 is in the order of $0.04a$, and depends on in which direction the origin is approached. This does not mean that the constitutive relation is multivalued or even anisotropic at $\boldsymbol{k} = \boldsymbol{0}$, since the factor β_1 should be multiplied by $\mathrm{i}\boldsymbol{k}\times$ which decreases to zero as $|\boldsymbol{k}| \to 0$. At $\boldsymbol{k} = \boldsymbol{0}$ only the parameters ϵ and μ contribute to the constitutive relation, and these do not depend on the direction the origin is approached in. We also notice a substantial increase in β_1 and β_2 as $\boldsymbol{k}a = (\pi, 0, 0)$ is approached, with peak values at $\beta_1 = \beta_2 = 0.78a$. Due to symmetry, this behavior repeats for $\boldsymbol{k}a = (0, \pi, 0)$ and $(0, 0, \pi)$.

To summarize, not even the Drude-Born-Fedorov model seems to be fully suitable for modeling this microstructure. For small $\boldsymbol{k}a$, *i.e.*, when the applied wavelength is very long compared to the unit cell, we rather have

$$\langle \widetilde{\boldsymbol{D}} \rangle = \epsilon(\langle \widetilde{\boldsymbol{E}} \rangle + \beta_0 \mathrm{i}\boldsymbol{k} \times \langle \widetilde{\boldsymbol{E}} \rangle) \tag{5.7}$$

$$\langle \widetilde{\boldsymbol{B}} \rangle = \mu \langle \widetilde{\boldsymbol{H}} \rangle \tag{5.8}$$

where β_0 depends on the direction of $\boldsymbol{k}$, being minimal along the principal directions of the unit cell and maximal along the diagonal. This looks more like Born's original model [4, 5]. The dependence of β_0 on direction does not contradict the isotropy of the unit cell geometry, since as soon as $\boldsymbol{k} \neq \boldsymbol{0}$, there is a preferred direction in the material which is not necessarily aligned with the periodicity. Isotropy for $\boldsymbol{k} \neq \boldsymbol{0}$ may be recovered in a random medium.

6 Conclusions

We have demonstrated that when using only real permittivities and permeabilities, there can be no coupling between electric and magnetic fields in the effective material parameters, even in the case of finite scale difference. The argument used is based on a particular symmetry due to the lossless medium, and breaks down as soon as we introduce a finite conductivity in the problem. However, it can be expected that the possible coupling due to small losses is weak.

Allowing for spatial dispersion, a chiral effect may appear as a gyrotropic part of the effective material tensor. According to the homogenization formalism used here, a lossless isotropic chiral material seems to be best modeled with a modified Drude-Born-Fedorov model. For small wave vectors, this model couples the circulation of

the electric field to the electric polarization but leaves the magnetic field without the corresponding coupling, which is Born's original model [4, 5]. The strength of the coupling in this low frequency limit depends on the propagation direction, being minimal along the principal directions of the unit cell, and maximal along the diagonal. Isotropy may be recovered in a random mixture, since then all directions are equal, even for finite wave vectors.

References

[1] H. Ammari, M. Laouadi, and J.-C. Nédélec. Low frequency behavior of solutions to electromagnetic scattering problems in chiral media. *SIAM J. Appl. Math.*, **58**(3), 1022–1042, 1998.

[2] A. Bensoussan, J. L. Lions, and G. Papanicolaou. *Asymptotic Analysis for Periodic Structures*, volume 5 of *Studies in Mathematics and its Applications*. North-Holland, Amsterdam, 1978.

[3] F. Bloch. Über die Quantenmechanik der Electronen in Kristallgittern. *Z. Phys.*, **52**, 555–600, 1928.

[4] M. Born. Über die natürliche optische Aktivität von Flüssigkeiten und Gasen. *Physik. Zeitschr.*, **XVI**, 251–258, 1915.

[5] M. Born. Über die natürliche optische Aktivität der Kristalle. *Zeitschrift für Physik*, **8**(1), 390–417, 1922.

[6] D. Cioranescu and P. Donato. *An Introduction to Homogenization*. Oxford University Press, Oxford, 1999.

[7] C. Conca, R. Orive, and M. Vanninathan. Bloch approximation in homogenization and applications. *SIAM J. Math. Anal.*, **33**(5), 1166–1198, 2002.

[8] D. C. Dobson, J. Gopalakrishnan, and J. E. Pasciak. An efficient method for band structure calculations in 3D photonic crystals. *Journal of Computational Physics*, **161**(2), 668–679, 2000.

[9] G. Floquet. Sur les équations différentielles linéaries à coefficients périodique. *Ann. École Norm. Sup.*, **12**, 47–88, 1883.

[10] V. V. Jikov, S. M. Kozlov, and O. A. Oleinik. *Homogenization of Differential Operators and Integral Functionals*. Springer-Verlag, Berlin, 1994.

[11] S. G. Johnson and J. D. Joannopoulos. Block-iterative frequency-domain methods for Maxwell's equations in a planewave basis. *Opt. Express*, **8**(3), 173–190, 2001.

[12] C. Kittel. *Introduction to Solid State Physics*. John Wiley & Sons, New York, 6 edition, 1986.

[13] A. Lakhtakia, V. K. Varadan, and V. V. Varadan. *Time-Harmonic Electromagnetic Fields in Chiral Media*, volume 335 of *Lecture Notes in Physics*. Springer-Verlag, New York, 1989.

[14] M. Lassas. The essential spectrum of the nonself-adjoint Maxwell operator in a bounded domain. *J. Math. Anal. Appl.*, **224**, 201–217, 1998.

[15] I. V. Lindell, A. H. Sihvola, S. A. Tretyakov, and A. J. Viitanen. *Electromagnetic Waves in Chiral and Bi-isotropic Media*. Artech House, Boston, London, 1994.

[16] K. F. Lindman. Om en genom ett isotropt system av spiralformiga resonatorer alstrad rotationspolarisation av de elektromagnetiska vågorna. *Översigt af Finska Vetenskaps-Societetens förhandlingar, A. Matematik och naturvetenskaper*, **LVII**(3), 1–32, 1914–1915.

[17] K. F. Lindman. Über eine durch ein isotropes System von spiralformigen Resonatoren erzeugte Rotationpolarisation der elektromagnetischen Wellen. *Ann. d. Phys.*, **63**(4), 621–644, 1920.

[18] G. W. Milton. *The Theory of Composites*. Cambridge University Press, Cambridge, U.K., 2002.

[19] R. C. Morgan and I. Babuška. An approach for constructing families of homogenized equations for periodic media. I: an integral representation and its consequences. *SIAM J. Math. Anal.*, **22**(1), 1–15, January 1991.

[20] R. C. Morgan and I. Babuška. An approach for constructing families of homogenized equations for periodic media. II: properties of the kernel. *SIAM J. Math. Anal.*, **22**(1), 16–33, January 1991.

[21] F. Santosa and W. W. Symes. A dispersive effective medium for wave propagation in periodic composites. *SIAM J. Appl. Math.*, **51**(4), 984–1005, 1991.

[22] D. Sjöberg. Homogenization of dispersive material parameters for Maxwell's equations using a singular value decomposition. *Multiscale Modeling and Simulation*, **4**(3), 760–789, 2005.

[23] D. Sjöberg, C. Engström, G. Kristensson, D. J. N. Wall, and N. Wellander. A Floquet-Bloch decomposition of Maxwell's equations, applied to homogenization. *Multiscale Modeling and Simulation*, **4**(1), 149–171, 2005.

[24] S. Torquato. *Random Heterogeneous Materials: Microstructure and Microscopic Properties*. Springer-Verlag, Berlin, 2002.